

# Effect of pH on Corrosion Inhibition of Steel by Polyaspartic Acid

D.C. Silverman, D.J. Kalota, and F.S. Stover\*

## ABSTRACT

*Polyaspartic acid, a polymeric form of aspartic acid ( $C_4H_7NO_4$ ), was examined as a corrosion inhibitor for steel as a function of pH, temperature, and hydrodynamic conditions. The temperature ranged from 25°C to 95°C, and the concentration ranged from < 1 wt% to ~ 10 wt%. Experimental procedures included electrochemical impedance spectroscopy (EIS), the rotating cylinder electrode (RCE), and coupon immersion. At low to neutral pH values, polyaspartic acid increased the corrosion rate of steel. At high pH (< ~ 10), polyaspartic acid was a reasonably robust corrosion inhibitor. Between pH 7 and 10, corrosion in the presence of polyaspartic acid was a complex function of temperature, concentration, water quality, and hydrodynamic conditions. By combining corrosion potential measurements with speciation diagrams obtained by titration, a reasonably cohesive explanation of the behavior was developed.*

**KEY WORDS:** *aspartic acid, biodegradable inhibitors, electrochemical impedance spectroscopy, immersion test, inhibition, iron, polarization resistance, polyaspartic acid, rotating cylinder electrode, steel, water treatment*

## INTRODUCTION

One type of corrosion inhibitor for steel that has aroused interest is the amino acid. Environmental restrictions are being placed on a number of common inorganic inhibitors (e.g., chromates),<sup>1</sup> and alternatives are required. Amino acids, if they show promise,

would be biodegradable and might avoid at least some environmental restrictions. Recently, several papers have suggested that some amino acids can function as corrosion inhibitors for iron and steel. In a rather exhaustive study, Hluchan, et al., examined the behavior of 22 amino acids as potential corrosion inhibitors for iron in strong acid (1 M hydrochloric acid [HCl]).<sup>2</sup> They found that the longer the hydrocarbon chain or the greater the number of additional amino groups was, the greater the corrosion inhibition was. Amino acids with shorter chains (e.g., glycine [ $C_2H_5O_2N$ ], aspartic acid [ $C_4H_7NO_4$ ], and glutamic acid [ $C_5H_9O_4N$ ]) showed only about a 50% reduction in corrosion rate as estimated by corrosion currents.

One important application area is the corrosion inhibition of steel at near neutral pH ( $5 < \text{pH} < 9$ ). Ramakrishnaiah measured the corrosion of steel in a number of amino acids in sodium chloride (NaCl) solutions at pH 8.<sup>3</sup> The goal actually was to examine the effects of biological compounds that might interact with steel when bacteria, algae, and fungi are present. While some amino acids were able to decrease corrosion, others such as aspartic acid actually seemed to accelerate corrosion. In no case was the corrosion rate reduced enough so that any of the amino acids would be capable of acting as a practical corrosion inhibitor.

In a recent patent, various amino acids and their salts at very high concentration were found to prevent the atmospheric corrosion of iron panels.<sup>4</sup> The panels were dipped in solutions containing ~ 20 wt% of the amino acid and then were hung indoors. No corrosion was observed. Atmospheric condensate

Submitted for publication September 1994; in revised form, March 1995. Presented as paper no. 34 at CORROSION/95, March 1995, in Orlando, FL.

\* Monsanto Co., 800 N. Lindbergh Blvd., St. Louis, MO, 63167.

would be expected to have a slightly acidic pH (~ 5.5).<sup>5</sup> Though the amino acid concentration was much higher than the 100 ppm in the previous study,<sup>3</sup> the difference in results suggests that pH may play a significant role in the ability of some amino acids to affect corrosion. This influence also is suggested by the fact that these amino acids have more than one acid-base equilibrium. The effect of multiple acid-base equilibria on corrosion has been examined more closely with respect to aspartic acid.<sup>6</sup> In that study, aspartic acid was found to change from a corrosion inhibitor to a corrosion accelerator as the pH dropped from above the highest acid-base constant (~ 9.5 to 10) to below it. This change in behavior was fairly sharp and occurred across the entire temperature range studied (25°C to 95°C). Coincident with that effect was a decrease in the corrosion potential by several hundred millivolts, with the lower potential being associated with the more corrosive condition.

Associated with that study was a brief examination of the effect on corrosion by polyaspartic acid, a polymerized form of aspartic acid.<sup>7</sup> Results suggested that steel corrosion was affected in a manner similar to that in the presence of aspartic acid. The rate increased as the pH dropped below ~ 10. However, Mueller, et al., reported that polyaspartic acid at low concentrations can function as a corrosion inhibitor for steel in seawater between pH 8 and 9.<sup>8</sup> This result seems to contradict that reported for polyaspartic acid and possibly those reported for aspartic acid at the same pH as above.<sup>9</sup> However, the inhibition efficiency was low, which suggests that the inhibition was incomplete.

The purpose of this study was to examine in more detail the effect of pH on polyaspartic acid acting as a corrosion inhibitor for steel across the pH range of 3.5 to 12 and the temperature range of 25°C to 90°C. Electrochemical impedance spectroscopy (EIS), the rotating cylinder electrode (RCE), and coupon immersion tests were combined to estimate the corrosion rate and to examine effects of agitation on the way steel passivates. In addition, titration curves were generated to establish the points at which the molecule would be ionized fully and to examine if the degree of ionization and its effect on complexation with iron could aid in explaining the observed corrosion characteristics.

## EXPERIMENTAL

The polyaspartic acid was prepared from aspartic acid by a proprietary thermal method. Its peak molecular weight was 9,200. The molecular weights

were determined by gel permeation chromatography using polyethylene glycol as the standard. C1018 steel (UNS G10180)<sup>(1)</sup> was used for all corrosion experiments. The electrodes were presanded using 600-grit silicon carbide (SiC) paper. The EIS apparatus, the algorithm for generating the impedance spectra, the algorithm for curve-fitting the results, the RCE apparatus, and the electrode geometry have been described in detail elsewhere.<sup>10-12</sup>

The impedance spectra were generated as a function of fluid rotation rate at 200 rpm, 1,000 rpm, and 2,000 rpm. The electrodes were rotated at 200 rpm during the entire experiment except for 1-h excursions to 1,000 rpm and 2,000 rpm each day. Spectra were generated at pH = 5, 8.5, and 10 at 35°C and at pH = 10 at 90°C. Two qualities of water were used, deionized water and a more aggressive water with a composition of 1.32 g calcium sulfate dehydrate (CaSO<sub>4</sub>·2H<sub>2</sub>O), 0.705 g magnesium chloride hexahydrate (MgCl<sub>2</sub>·6H<sub>2</sub>O), 0.190 g sodium bicarbonate (NaHCO<sub>3</sub>), 1.7 g sodium sulfate (Na<sub>2</sub>SO<sub>4</sub>), and 3,094 g water. The water is labeled "corrosive" throughout the text.

The immersion tests were run in ~ 750 mL (25.36 oz) of solution containing various concentrations of polyaspartic acid. The coupons used in these experiments were presanded using 120-grit SiC paper. Water-saturated air flowed through all of the vessels. The immersion experiments lasted ~ 168 h. The jars were placed in a constant temperature bath to maintain one of two temperatures, 30°C or 90°C. The pH was adjusted at room temperature to the appropriate level using reagent-grade sodium hydroxide (NaOH) or sulfuric acid (H<sub>2</sub>SO<sub>4</sub>) as appropriate. Duplicate exposures were run in many instances. The pH was measured at both room temperature and at 90°C in those experiments involving elevated temperatures. A somewhat more intensive examination was made for pH values between 8.5 and 10. In those cases, the pH was adjusted daily during the duration of the experiment. Three types of water were used, deionized water, St. Louis County, Missouri, tap water (23 ppm Ca<sup>2+</sup>, < 2 ppm Cu<sup>2+</sup>, < 1 ppm Fe<sup>3+</sup>, 20 ppm to 21 ppm Mg<sup>2+</sup>, < 5 ppm P as phosphate, and < 0.9 ppm Zn<sup>2+</sup>), and the more corrosive water described above.

The titrations of the polyaspartic acid were done by diluting from a base stock of a 28 wt% solution of the sodium salt. The pH titrations were performed on a Brinkmann 636<sup>†</sup> titrator using a 0.01 N NaOH/0.09 N sodium perchlorate (NaClO<sub>4</sub>) titrant and a Fisher Scientific Model 13-620-90<sup>†</sup> combination electrode with 3 M NaCl/0.5 M NaClO<sub>4</sub> reference filling solution. The titrant was standardized vs 5 mL (0.169 oz) 0.01 M primary standard-grade potassium hydrogen phthalate. After preliminary electrode calibration with pH 4 and pH 7 buffers, a final calibration in hydrogen ion was performed by titrating

<sup>(1)</sup> UNS numbers are listed in *Metals and Alloys in the Unified Numbering System*, published by the Society of Automotive Engineers (SAE) and cosponsored by ASTM.

<sup>†</sup> Trade name.

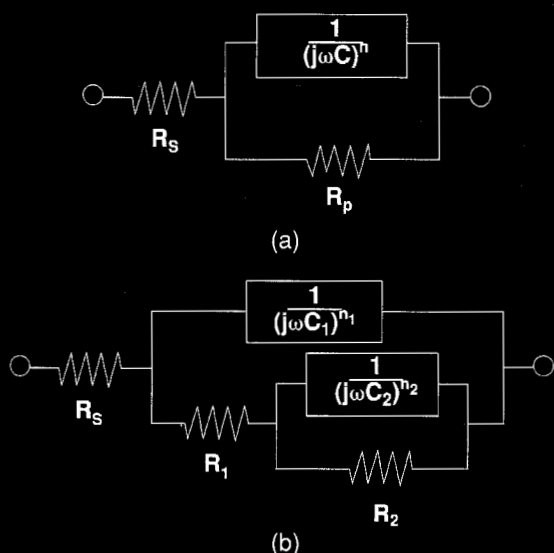


FIGURE 1. Analogous circuits used for EIS modeling: (a) simple charge transfer process and (b) 2 time constants as in imperfect coating or inhibitors.

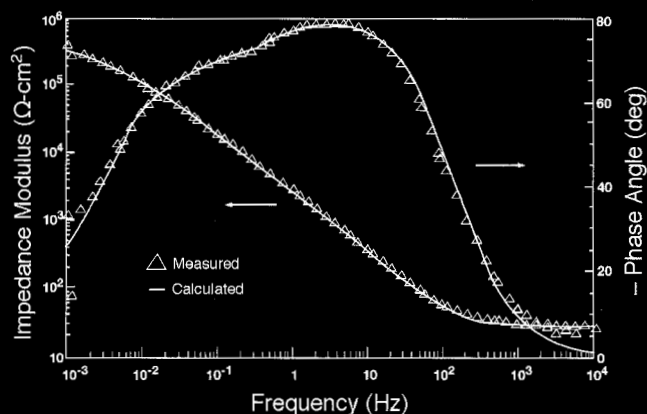


FIGURE 2. Impedance spectrum of steel in 3 wt% polyaspartic acid and deionized water, pH = 10, 35°C, 200 rpm.

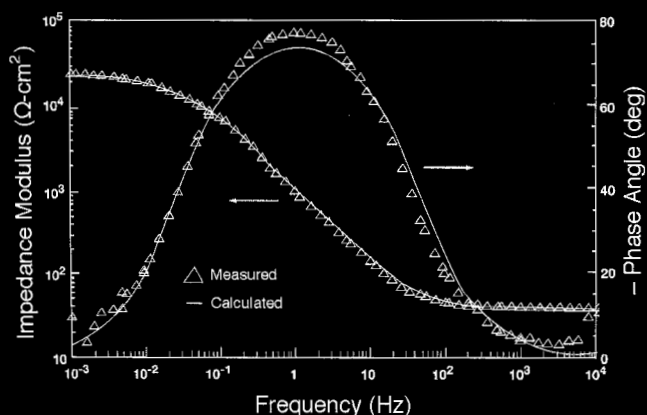


FIGURE 3. Impedance spectrum of steel in 3 wt% polyaspartic acid and deionized water, pH = 8.5, 35°C, 200 rpm.

2 mL (0.068 oz) 0.01 M perchloric acid ( $\text{HClO}_4$ )/0.09 M  $\text{NaClO}_4$ .

The following titrations were performed in the monotonic mode with data taken every 0.2 mL (0.007 oz):

— 0.1 meq sodium polyaspartate ( $[\text{C}_4\text{H}_4\text{NO}_3\text{Na}]_x$ ) + 0.1 mM  $\text{HClO}_4$  to determine the  $\text{pK}_a$  values of polyaspartic acid,

— 0.05 mM ferrous sulfate ( $\text{FeSO}_4$ ) to examine qualitatively iron hydrolysis and hydroxide formation, and

— 0.1 meq sodium polyaspartate + 0.1 mM  $\text{HClO}_4$  + 0.0125, 0.025, or 0.05 mM  $\text{FeSO}_4$  to assess iron-polyaspartate complexation.

Initial volumes of all titrations were 10 mL (0.338 oz), and all solutions were adjusted to 0.1 N ionic strength by addition of  $\text{NaClO}_4$ .

## RESULTS

### Electrochemical

The impedance spectra were analyzed using the analogous circuits in Figure 1. The spectra were fitted using the software of Boukamp.<sup>13</sup> Figures 2 through 4 show the impedance results for 3 wt% (2.3 molal) polyaspartic acid at pH = 10, 8.5, and 5 at 35°C for rotation rates of 200 rpm. The impedance spectra at the higher rotation rates showed similar characteristics. The impedance spectra generated at 90°C and pH 10 looked identical to that at 35°C and pH 10. These experiments were in deionized water. The pH at 10 drifted slowly to more acidic values. At 35°C, it reached ~9.8 by the end of the experiment. At 90°C, it reached ~8.8 or so by the end of the experiment. Therefore, the spectra taken after 24 h of exposure were expected to have pH values close to those at the start. The impedance spectra generated at the higher pH values were fitted by using two relaxation time constants. The spectra generated at pH 5 required only one relaxation time constant.

The low-frequency time constant observed at pH 8.5 and 10 and the single relaxation time constant at pH 5 were assumed to be inversely proportional to the corrosion rate. This point was corroborated by comparing corrosion rates estimated from the mass loss of the electrode to those estimated from the impedance spectra using a Tafel constant of 0.025 V. The corrosion rates estimated from the impedance measurements were transformed into a time-averaged corrosion rate to compare to mass loss by assuming that each rate estimated from the impedance spectrum lasted from the time of measurement until the next measurement. The rates were multiplied by the number of hours assigned to that rate, summed together, and divided by the total time. These comparisons are shown in Table 1.

In view of the assumptions and the leakage observed in at least one experiment, the agreement

TABLE 1

Comparison Between Corrosion Rates Determined by Impedance vs Mass Loss in 3 wt% Polyaspartic Acid<sup>(A)</sup>

| Conditions     | Corrosion Rate (mm/y) |                      |
|----------------|-----------------------|----------------------|
|                | Impedance             | Mass Loss            |
| pH = 8.5, 35°C | $3.0 \times 10^{-1}$  | 1.1                  |
| pH = 10, 35°C  | $5.0 \times 10^{-2}$  | $5.0 \times 10^{-1}$ |
| pH = 10, 90°C  | $3.0 \times 10^{-1}$  | $9.0 \times 10^{-1}$ |
| pH = 5, 35°C   | 57                    | 101                  |

<sup>(A)</sup> There was seepage of liquid behind the spacer which led to excess corrosion in the area not exposed directly to the fluid. This corrosion led to excess mass loss. The impedance estimate is expected to more closely reflect the time-averaged corrosion rate.

indicated the impedance spectra represented the corrosion processes. At pH 10, the capacitance of the high-frequency time constant was of the order of  $50 \mu\text{F}/\text{cm}^2$ , while that at pH 5 was much larger. This capacitance value approached that expected for the double layer. Also, the phase angle plot in Figure 4 was broad, and the maximum approached  $90^\circ$ . These characteristics are observed often on highly passive surfaces and suggest very capacitive behavior.

Figure 5 shows a plot of the reciprocal of the polarization resistance assumed to be related to the corrosion rate as derived from the circuit model as a function of time and rotation rate for immersion in deionized water. This type of plot shows how the corrosion rates change with time and the relationship among the corrosion rates without relying on the assumed Tafel slopes. The corrosion rate was independent of rotation rate when the steel was passivated completely at the high pH. At pH 5, where the corrosion rate was high, a sensitivity to fluid motion was observed.

Impedance spectra (not shown) were generated for 3 wt% polyaspartic acid at pH = 8.5 and 10 in the more corrosive water. The polarization resistances in the more corrosive water were much smaller than at comparable pH values in deionized water, which indicated increased corrosion. Figures 6 and 7 are similar to Figure 5 and compare the behavior of the polarization resistance for polyaspartic acid in deionized water and the more corrosive water as a function of time and rotation rate at pH 8.5 (Figure 6) and pH 10 (Figure 7). The corrosion rates in each water initially differed by  $\sim 1$  order of magnitude. However, this difference decreased with time. The corrosion rates in both types of water approached each other under the dynamic conditions in the RCE. The corrosion rates at pH 8.5 were greater than at pH 10.

### Immersion Experiments

A number of immersion experiments were run to examine the corrosiveness of polyaspartic acid in water. The experiments were concentrated in two regimes, the pH range between 8 and 10, in which

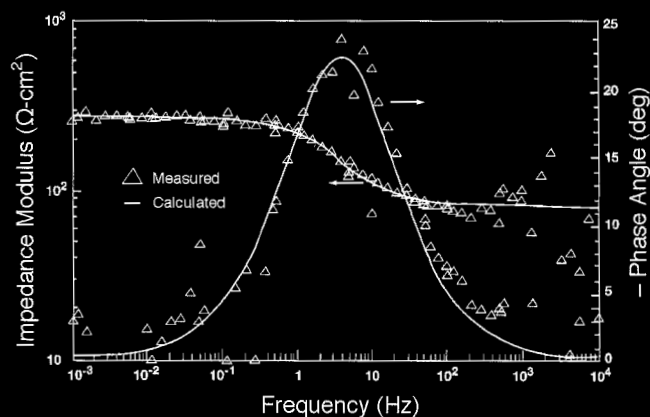


FIGURE 4. Impedance spectrum of steel in 3 wt% polyaspartic acid and deionized water, pH = 5, 35°C, 200 rpm.

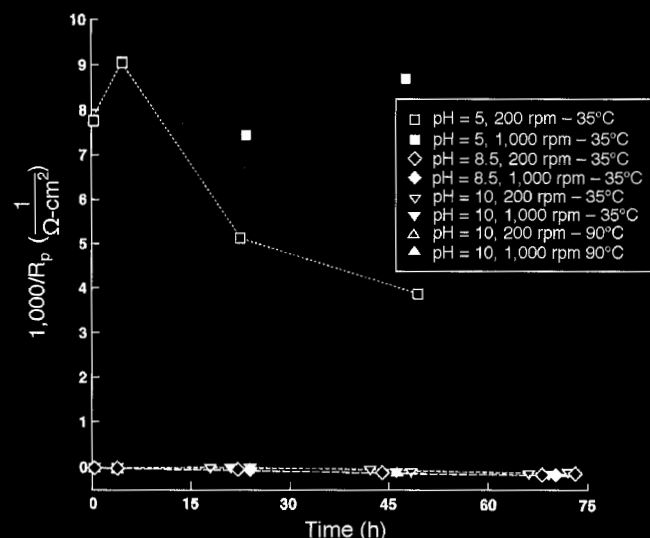


FIGURE 5. Corrosion of steel in 3 wt% polyaspartic acid in deionized water as a function of time and rotation rate.

the corrosion rate was reported previously to increase rather rapidly with falling pH, and in the pH between 3.5 and 7, in which the corrosion rate was high but left the surface very smooth, indicating uniform corrosion.

Though a large number of immersion experiments were run, only a few of the results are reported in detail. For these experiments, a temperature of  $50^\circ\text{C}$  was used to simulate very warm, ambient conditions and to supplement the previous results at  $35^\circ\text{C}$  and  $90^\circ\text{C}$ . The first experiments focused on the pH range of 8.5 to 10 to examine more closely the reports of the ability of polyaspartic acid to inhibit corrosion in the pH range below 10. A series of immersion tests were run at  $50^\circ\text{C}$  in two types of water, the corrosive water and St. Louis County, Missouri, tap water. The experiments were run by immersing C1018 steel corrosion coupons in the

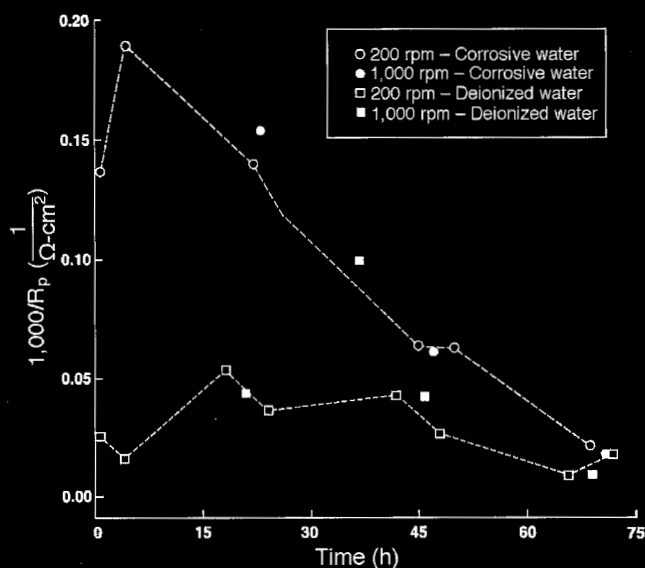


FIGURE 6. Corrosion of steel in 3 wt% polyaspartic acid at pH 8.5 as a function of water quality, time, and rotation rate at 35°C.

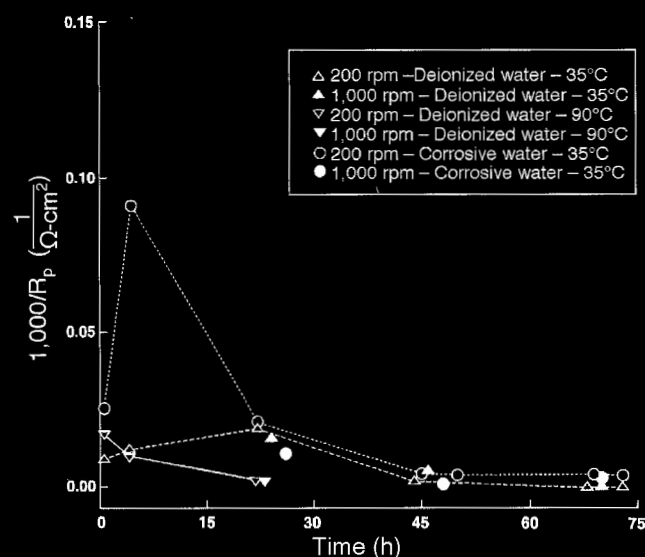


FIGURE 7. Corrosion of steel in 3 wt% polyaspartic acid at pH 10 as a function of water quality, time, and rotation rate.

liquid. Air was sparged gently into the solutions after it passed through deionized water to saturate it. The pH was checked and adjusted daily. Results are shown in Figures 8 and 9.

Immersion experiments also were run to examine corrosion at lower pH (between 3.5 and 7, which was a region in which polyaspartic acid might be expected to complex with iron). Such complexing has been found to greatly increase the corrosion rate of steel in other types of environments.<sup>14</sup> Figure 10 shows the results for a series of immersion experiments at pH 3.5 and 5 at 35°C and 93°C. Deionized water was used for the experiments. Though the corrosion rates

were high, the surface texture was smooth, which indicated corrosion was uniform in this pH range.

## DISCUSSION

Results indicated polyaspartic acid has corrosion inhibition properties at high pH (> ~ 10). This inhibiting ability at higher pH is similar to that noted previously for aspartic acid.<sup>6-7</sup> Polymerization of aspartic acid to polyaspartic acid would eliminate one of the two carboxylic acid groups from each molecule. This observation suggests that the corrosion inhibition at high pH does not depend on two carboxylic acid groups being fully ionized on each moiety.

One difference between the behavior of aspartic acid and polyaspartic acid as a function of pH is the fuzziness of the pH boundary between polyaspartic acid acting as a corrosion inhibitor and an accelerator. This pH boundary is not defined as sharply as for aspartic acid.<sup>6</sup> In the case of aspartic acid, the corrosion rate increased rapidly as the pH decreased only a small distance below ~ 9.5. Polyaspartic acid showed greater corrosion inhibition than aspartic acid in the pH range between 8 and 10, but the inhibition was not robust in that corrosion was a much stronger function of concentration and flow conditions. This point was reflected in the fact that under dynamic conditions, corrosion tended to be lower and more uniform in this pH range (Table 1 and Figures 5 through 7), while under static conditions, regions of nonuniform corrosion began to appear (Figures 8 and 9), and the corrosion rate began to rise much more rapidly as pH dropped below 10.

Differences in the titration curves of these two acids suggested one possible explanation. Figure 11 shows that two distinct equivalence points exist for aspartic acid in agreement with the two higher pK values for this acid.<sup>14</sup> Such sharp equivalence points are absent for polyaspartic acid. The two breaks are replaced by one very broad curve that extends over 6 to 7 pH units. Whereas, aspartic acid reached full deprotonation at pH of ~ 11, polyaspartic acid reached full deprotonation at pH of ~ 7. However, complete corrosion inhibition still was not achieved at this low pH. This observation strongly suggested that the need for complete deprotonation is not the total explanation for corrosion inhibition by polyaspartic acid.

Figure 12 shows a titration curve for polyaspartic acid as pH vs milliliters of titrant between pH 3 and 6. The curve was established by titrating a 0.1 meq sodium polyaspartate solution containing 0.1 mM HClO<sub>4</sub>. The titration curve was modeled successfully by assuming the presence of four pK values. The program "PKAS" by Motekaitis and Martell was used for the calculation.<sup>15</sup> The only assumption made was that the equivalent weight of the sodium polyaspartate was 137. Agreement

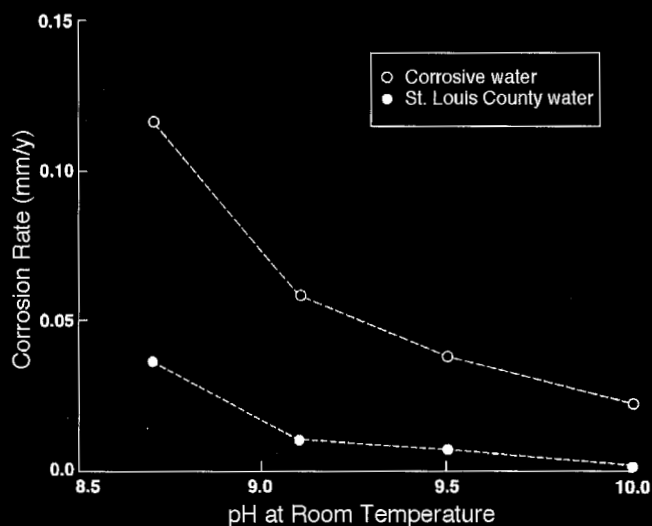


FIGURE 8. Corrosion rate of steel by immersion tests in 10 wt% polyaspartic acid at 50°C as a function of pH and water quality.

between a model that assumed four pKa values and the experimental results did not necessarily mean that only four pK values existed. The results meant that the acidity of the polyaspartate molecule could be modeled as if there were four distinct acid moieties. The concentration based formation constants written as  $\log_{10}K$  for the reaction  $\text{Ligand} + n\text{H}^+ = \text{H}_n\text{Ligand}$  were 5.4, 4.3, 3.6, and 2.2 for  $n = 1, 2, 3, 4$  respectively. Above pH of ~ 6 to 7, the polyaspartate molecule could be modeled as if its hydrogen ions that contribute to its acidity were removed.

The most apparent difference between the acid-base behavior of the two acids was the absence of a pK value in the basic pH region for polyaspartic acid. This basic pK is associated with deprotonation of the amine group. Such a reaction was absent in polyaspartic acid. Assuming that acidity plays a role in the corrosion inhibition properties of these acids, this difference supported differences in the corrosion inhibition properties found for these acids, especially above a pH of 7.

With this pKa model in hand, solutions containing sodium polyaspartate, sodium polyaspartate and iron introduced as  $\text{FeSO}_4$ , and a solution of  $\text{FeSO}_4$  alone were titrated. The goal was to estimate the types of iron aspartate ligands that might be present especially in the acid pH range. The presence of iron increased the required amount of titrant for a given pH, indicating binding of iron with polyaspartate ion. No special precautions were used to eliminate oxygen. Therefore, since the titrations were performed slowly, all complexed iron should have been ferric, and the results could reflect Fe(III) reacting with the polyaspartate molecule.

The stability constants in the form  $B_{\text{mhl}}$  (where  $B_{\text{mhl}} = [\text{M}_m\text{L}_l\text{H}_h]/[\text{M}]^m[\text{L}]^l[\text{H}]^h$  and M, L, and H are the metal (Fe), ligand (one polyaspartate repeat unit),

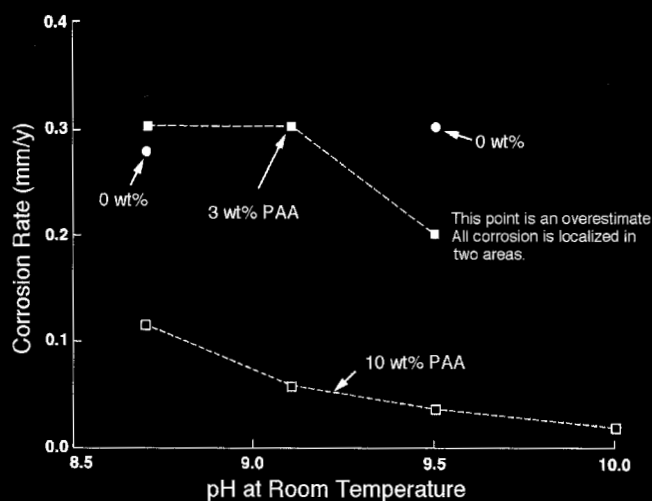


FIGURE 9. Corrosion rate of steel by immersion tests at 50°C in corrosive water as a function of polyaspartic acid concentration and pH.

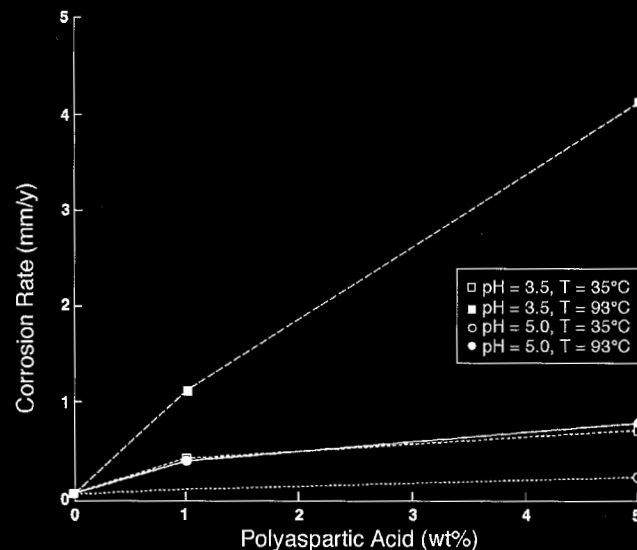


FIGURE 10. Corrosion rate of steel by immersion tests at low pH as a function of pH and temperature.

and hydrogen, respectively, were estimated from the titration curve using the program "BEST" by Motekaitis and Martell.<sup>16</sup> The best fit was found to contain the stoichiometry, written as  $\text{MLH}$ , of 110, 111, 112, and 11(-2) where (-2) means two hydroxides. The species would be  $\text{Fe}(\text{PAA})$ ,  $\text{FeH}(\text{PAA})$ ,  $\text{FeH}_2(\text{PAA})$ , and  $\text{Fe}(\text{OH})_2(\text{PAA})$ , where PAA signifies the polyaspartate moiety. The charges on the above species have not been included. Figure 13 shows a speciation plot based on the estimated stability constants and the species. The "110" species showed a maximum at pH 5.7, and the noncomplexed iron was present to ~ pH 6.5. The model was tested by preparing solutions which contained a 1:4 mM/meq ratio of Fe to PAA and the pH was adjusted to 5.7, 6.5, and

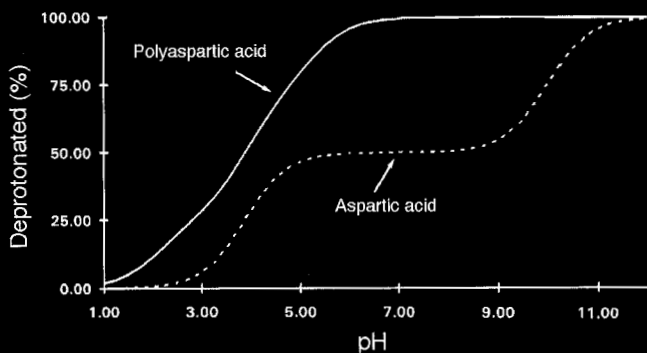


FIGURE 11. Titration curve showing percent deprotonation vs pH for L-aspartic and polyaspartic acids.

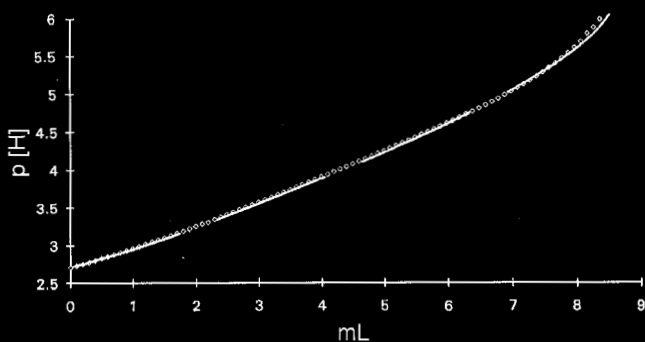


FIGURE 12. Fit of model assuming 4 values of  $pK$  for polyaspartic acid. The points are measured, and the lines are the model.

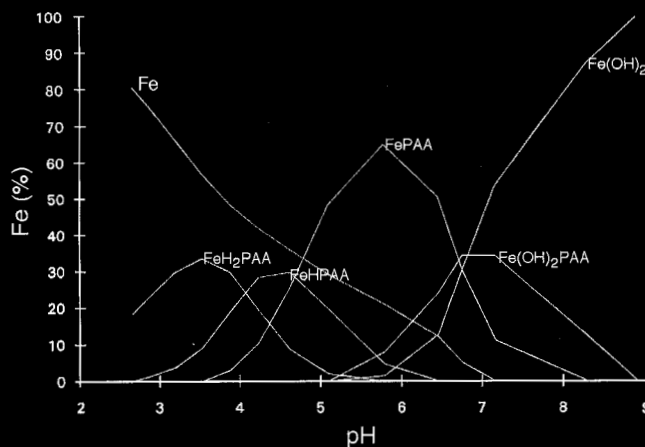


FIGURE 13. Iron-polyaspartic acid complexation species as a function of pH.

9.5, which represented levels of maximum formation of  $FePAA$ ,  $Fe(OH)_2PAA$ , and  $Fe(OH)_2$ . After 24 h, the solutions at lower pH were clear and that at the higher pH was cloudy, strongly suggesting the presence of species with an Fe:PAA ratio of 1:4 consistent with Figure 13.

Combining Figure 13 as a model of the speciation of polyaspartic acid and iron and the corrosion

potential-vs-pH information in Table 2 and Figure 1 of Kalota, et al., led to a plausible explanation for the complicated interaction of polyaspartic acid with iron or steel.<sup>6</sup> As in the case of aspartic acid, the behavior of the corrosion potential for steel in the presence of polyaspartic acid indicated an ability of the polymer to passivate the surface at elevated pH by shifting the potential in the noble direction relative to the hydrogen/hydrogen ion equilibrium. At lower pH values (e.g., pH 5), the corrosion potentials remained near the hydrogen/hydrogen ion equilibrium.

Figure 13 shows the type of chemistry that could lie behind these shifts in corrosion potential. Below pH of  $\sim 7$ , various iron-polyaspartate complexes could form. Below pH of  $\sim 5$ , these species had one or two hydrogen ions associated with them. Corrosion rates were very high and uniform in this pH range. These observations suggested that iron-aspartate complexes accelerated the corrosion of iron at low pH and caused the corrosion potentials to lie near the  $H_2/H_2O$  boundary. Very likely,  $Fe(II)$  was the stable state of iron being complexed to the polyaspartate moiety since the corrosion potentials were near the hydrogen line. Complexes between iron and an organic acid have been shown previously to increase corrosion.<sup>17</sup>

At higher values of pH, hydrogen ions first were eliminated from the complex. Corrosion rates may still have remained high because of the complexation with iron. However, at pH of  $\sim 7$ , the complex was found to contain hydroxyl ions, not hydrogen ions. Finally, at still higher pH values, the polyaspartate ion no longer complexed with iron. This change in chemistry was accompanied by an increase in corrosion potential into a region of stability of iron oxides such as  $Fe_2O_3$ ,  $FeOOH$ , and  $Fe_3O_4$ .<sup>6</sup>

In the pH range between 7 and 10, corrosion in the presence of polyaspartic acid was a complex function of temperature, inhibitor concentration, water quality, and hydrodynamics. For example, Figure 8 shows that steel corroded when it was exposed to corrosive water containing 3 wt% polyaspartic acid at pH 8.5. However, when controlled hydrodynamic conditions were used, as in the RCE, such corrosion decreased until it was coincident with that in a solution made from deionized water (Figure 7). This beneficial effect of fluid velocity has been noted previously for other inhibitors that tend to shift the potential in the noble direction.<sup>18</sup> By contrast, water quality had almost no effect at pH 10. The corrosion rate was a function of the combined variables of pH, water quality, and hydrodynamics in the pH range of at least 8.5 to 10.

These observations were consistent with the corrosion rate behavior and chemistry. First the corrosion potential was rising in this pH range, from a value near the  $H_2/H_2O$  boundary to a value in the region of stability of iron oxide ( $Fe_2O_3$ ). This rise coin-

cides in Figure 13 with the disappearance first of an Fe(PAA) ligand and finally of an Fe(OH)<sub>2</sub>(PAA) ligand. In the pH range of 7 to 10, iron could be associated with both polyaspartate and with oxygen or hydroxide. Corrosion depended on which species was formed at the surface. The ability of the species to interact with the surface depended upon temperature and the ability of the species to get to the surface (hydrodynamics). Indeed, adjacent areas of the surface could have interacted with polyaspartate and with water to set up only local galvanic cells. Such an occurrence would explain the incomplete corrosion protection noted in Figure 9 at pH 9.5.

Finally, as the pH increased above ~ 10, polyaspartate ions no longer formed stable complexes with iron, at least complexes in solution like those formed at lower pH. However, some type of interaction with the surface must have been present because of the large, stable, 400-mV increase in corrosion potential that occurred relative to the hydrogen/hydrogen ion equilibrium at a pH of 10 shown in Table 2. Low corrosion rates were observed when the pH is > 9.5 to 10. Fluid hydrodynamics had no effect on corrosion. The chemistry in Figure 13 was consistent with this behavior at high pH. An iron-hydroxide complex was the only compound predicted to be present. Though iron hydroxide cannot form a passive layer, its prediction in the presence of polyaspartate supported the concept of a passivating iron oxide surface structure being stable at higher pH and no iron-polyaspartate solution complexes being present. At this point, the mechanism by which polyaspartate ions aid in stabilizing this passivity is unknown.

## CONCLUSIONS

- ❖ Polyaspartic acid acts as a corrosion accelerator at pH < ~ 7 and as a corrosion inhibitor for iron and steel at pH > ~ 10 for concentrations in the range of 1 wt% to 10 wt%.
- ❖ In the pH range between 7 and 10, the effect of polyaspartic acid on the corrosion of iron and steel is a complex function of hydrodynamics, temperature, concentration, and water quality.
- ❖ The behavior of polyaspartic acid with respect to steel corrosion could be explained by its ability to complex with iron as a function of pH. At lower pH values, iron-polyaspartate complexes were stable. At higher pH values, no such complexes were predicted. The corrosion potential was raised to a range in which iron oxides were stable thermodynamically.

## ACKNOWLEDGMENTS

The authors acknowledge the assistance of H. Thompson, J. Carrico, and G. Dinkelkamp.

TABLE 2

Corrosion Potentials of Various Polyaspartic Acid Solutions

| Solution Composition<br>(2 wt% Polyaspartic in:) | Time<br>(h) | Corrosion Potential<br>(V <sub>SCE</sub> ) |
|--|-------------|--|
| Deionized water<br>pH = 5, 35°C                  | 24          | -0.602                                     |
|  | 48          | -0.568                                     |
| Deionized water<br>pH = 8.0, 35°C                | 24          | -0.354                                     |
|  | 48          | -0.362                                     |
| Deionized water<br>pH = 10.0, 35°C               | 24          | -0.347                                     |
|  | 48          | -0.236                                     |
| Deionized water<br>pH = 10.0, 90°C               | 24          | -0.239                                     |
|  | 48          | -0.136                                     |
| Corrosive water<br>pH = 8.5, 35°C                | 24          | -0.381                                     |
|  | 48          | -0.301                                     |
| Corrosive water<br>pH = 10.0, 35°C               | 24          | -0.270                                     |
|  | 48          | -0.200                                     |

(A) Potentials of the equilibrium  $H_2 + 2e \rightarrow 2H^+$  are  $-0.55 V_{SCE}$  at a hydrogen ion activity of  $10^{-5}$  (pH = 5),  $-0.76 V_{SCE}$  at a hydrogen ion activity of  $10^{-8}$  (pH = 8), and  $-0.85 V_{SCE}$  at a hydrogen ion activity of  $10^{-10}$  (pH = 10).

## REFERENCES

1. A.J. Freedman, "Cooling Water Treatment," in *Process Industries Corrosion*, eds. B.J. Moniz, W.J. Pollock (Houston, TX: NACE, 1986), p. 205.
2. V. Hluchan, B.L. Wheeler, N. Hackerman, *Werkst. Korros.* 39 (1988): p. 512.
3. K. Ramakrishnaiah, *Bull. Electrochem.* 2, 1 (1986): p. 7.
4. Nippon Kokoh Seishi, "Corrosion Inhibitor for (non) Ferrous Metals Contains Amines and Amino Acids or Their Salts," Japanese patent No. J50091546-A, July 22, 1975.
5. G.W. Whitman, R.P. Russell, V.J. Altieri, *Ind. Eng. Chem.* 16, 7 (1924): p. 665.
6. D.J. Kalota, D.C. Silverman, *Corrosion* 50, 2 (1994): p. 138.
7. D.J. Kalota, D.C. Silverman, "Process for Corrosion Inhibition of Ferrous Metals," U.S. patent No. 4,971,724, issued Nov. 20, 1990.
8. E. Mueller, C.S. Sikes, B.J. Little, *Corrosion* 49, 10 (1993): p. 829.
9. B.J. Little, C.S. Sikes, "Corrosion Inhibition by Thermal Polyaspartate," in *Surface Reactive Peptides and Polymers*, ACS Symp. Series 444, eds. C.S. Sikes, A.P. Wheeler (Washington, DC: ACS, 1989), p. 263.
10. D.C. Silverman, J.E. Carrico, *Corrosion* 44, 5 (1988): p. 280.
11. D.C. Silverman, *Corrosion* 40, 5 (1984): p. 220.
12. D.C. Silverman, "Corrosion Prediction from Circuit Models Application to Evaluation of Corrosion Inhibitors," in *Electrochemical Impedance: Analysis and Interpretation*, ASTM STP 1186, ed. J.R. Scully, D.C. Silverman, M.W. Kendig (Philadelphia, PA: ASTM, 1993), p. 192.
13. B. Boukamp, "Equivalent Circuit (EQUIV.PAS)," Version 3.97 with (80)2(87) Support, 1989.
14. L.G. Sillen, A.E. Martell, *Stability Constants of Metal-Ion Complexes*, Supplement No. 1, Special Publication No. 25 (London, England: The Chemical Society, Burlington House, 1971).
15. R.J. Motekaitis, A.E. Martell, *Canad. J. Chem.* 60 (1982): p. 168.
16. R.J. Motekaitis, A.E. Martell, *Canad. J. Chem.* 60 (1982): p. 2,043.
17. D.C. Silverman, *Corrosion* 44, 9 (1988): p. 606.
18. A.M. Shams El Din, A.M.K. Tag El Din, E.A. El Sum, *Metaux: Corrosion Industrie* 63, 752 (1988): p. 123.